ISSN: 2688-8645

Research on Denoising Methods for Bearing Fault Vibration Signals Based on Wavelet Analysis and Envelope Demodulation

Chenyang Gu

School of Mechanical Engineering, Xi'an Shiyou University, Xi'an Shaanxi, 710065, China

Abstract

Bearing vibration signals are often susceptible to environmental factors and measurement system interference during practical acquisition, resulting in low signal-to-noise ratios and difficulty in extracting fault features. To address this issue, this study investigates a denoising method for vibration signals based on wavelet analysis and envelope demodulation. First, the fundamental principles of wavelet threshold denoising and Hilbert envelope demodulation are introduced, and the influence of different thresholding strategies on denoising performance is analyzed. Subsequently, time-domain and frequency-domain analyses are performed on bearing acceleration vibration signals. The signals are processed using both wavelet threshold denoising and wavelet-based envelope demodulation denoising, and their denoising performances are comparatively evaluated. Results indicate that wavelet threshold denoising alone can suppress high-frequency noise to some extent, but residual noise remains. In contrast, combining envelope demodulation with subsequent wavelet denoising more effectively reduces high-frequency noise, enhances the rotational frequency and related characteristic frequency components of the bearing, and significantly improves the signal-to-noise ratio and feature distinguishability. The proposed method provides an effective signal preprocessing approach for bearing fault feature extraction and condition monitoring.

Keywords

Bearing Vibration Signal; Wavelet Denoising; Envelope Demodulation Hilbert Transform; Fault Feature Extraction.

1. Introduction

Bearings are critical components in mechanical systems, responsible for supporting and guiding rotating elements, ensuring smooth rotation of mechanical parts, and preventing excessive friction or resistance. By reducing friction between rotating components, bearings decrease energy loss in mechanical systems, thereby improving system efficiency, reducing energy consumption, and extending the service life of mechanical components. In addition, bearings play an important role in cushioning and vibration damping within mechanical systems, helping to control vibration and noise levels. Stable mechanical operation not only enhances workplace comfort but also effectively prevents accidents. The normal operation of bearings is vital for the stability and reliability of the entire mechanical system, while bearing faults may lead to performance degradation or even severe accidents. In critical areas such as industrial production lines or transportation, the safety of mechanical systems is directly related to the safety of personnel and equipment [1, 2]. Stable bearings ensure controllable system operation and effectively reduce the risk of accidents. Bearing failures can result in machinery downtime, thereby affecting production schedules. Timely bearing fault diagnosis and maintenance can prevent failures and improve the reliability of mechanical systems.

ISSN: 2688-8645

The Case Western Reserve University (CWRU) Bearing Data Center provides test signals for both healthy and faulty bearings. The experiments were conducted using a 2-horsepower Reliance Electric motor, with acceleration data measured both near and away from the motor bearings. Bearing faults were introduced using electrical discharge machining (EDM). Fault diameters ranged from 0.007 inches to 0.040 inches and were applied to the inner race, rolling elements, and outer race. The faulty bearings were reinstalled into the test motor, and vibration data were recorded under motor loads from 0 to 3 horsepower (motor speed ranging from 1797 rpm to 1720 rpm) [3].

Techniques such as wavelet analysis, empirical mode decomposition (EMD), and modulation envelope analysis are commonly used to reduce noise in interference signals [4, 5, 6]. Traditional denoising methods include optimal estimation, optimal filtering, and adaptive filtering approaches. In practical engineering applications, some signal information may be lost during filtering or signal distortion, potentially leading to diagnostic errors. Wavelet decomposition offers multi-resolution analysis with both time- and frequency-domain localization, enabling the extraction of useful information from raw signals. Noise and other interference components are primarily concentrated in the high-frequency domain; however, useful signal components may also be present in these frequencies. Wavelet packet transform (WPT), based on wavelet transform, decomposes the original signal by separately processing low- and high-frequency components. After thresholding the wavelet packet coefficients and reconstructing the signal, WPT provides greater flexibility and accuracy compared to traditional wavelet transform [7].

2. Principles of Denoising Methods for Bearing Vibration Signals

2.1. Wavelet Analysis Denoising Method

The wavelet packet threshold denoising method decomposes the signal at multiple scales and applies thresholding to high-frequency wavelet coefficients dominated by noise. This approach effectively removes noise while preserving the main energy and structural features of the signal. Since its introduction in the 20th century, wavelet analysis has gradually developed into an important tool in the field of signal processing and has been widely applied in practical engineering. Compared with traditional wavelet decomposition, wavelet packet denoising provides a more detailed decomposition across the entire frequency spectrum, effectively improving the frequency resolution in high-frequency components and mitigating the limited time resolution in low-frequency components, thereby significantly enhancing the time-frequency analysis capability of signals. This method allows reasonable reconstruction of the signal based on the characteristics of each sub-band while ensuring that the signal energy is not significantly lost. The core idea of the wavelet shrinkage denoising algorithm is thresholding of wavelet coefficients. By suppressing small coefficients dominated by noise, the algorithm achieves effective noise removal while maintaining good fidelity to the original signal features. In addition, the algorithm has a clear structure, is relatively simple to implement, and can be easily realized and promoted on numerical computing platforms such as MATLAB [5, 8, 9].

The continuous wavelet transform (CWT) of a signal $f(t) \in L^2(\mathbb{R})$ with respect to the wavelet basis $\psi(t)$ is expressed as:

$$WT_f(\alpha,\tau) = [f(t), \psi_{\alpha,\tau}(t)] = \frac{1}{\sqrt{\alpha}} \int_R f(t)\psi^* \left(\frac{t-\tau}{\alpha}\right) dt \quad (1)$$

In the equation, $\alpha > 0$ is the scaling parameter, which controls the width of the wavelet basis. $\tau \in \mathbb{R}$ is the translation parameter, which determines the position of the wavelet along the time axis. $\psi^*(\cdot)$ denotes the complex conjugate of the wavelet basis function. The wavelet transform essentially represents the inner product of the signal with a family of wavelet basis functions that have been scaled and translated, thereby enabling the extraction of local features of the

ISSN: 2688-8645

signal at different time scales. When the wavelet function satisfies the admissibility condition, the original signal can be reconstructed through the inverse wavelet transform, which is expressed as:

$$f(t) = \frac{1}{C_\psi}\int_0^{+\infty}\frac{d\alpha}{\alpha^2}\int_{-\infty}^{+\infty} WT_f(\alpha,\tau)\frac{1}{\sqrt{\alpha}}\psi(\frac{t-\tau}{\alpha})d\tau \quad (2)$$

C_ψ is the admissibility constant of the wavelet function. In practical engineering applications, the continuous wavelet transform is computationally intensive, and the discrete wavelet transform is commonly used for signal analysis. Taking a three-level wavelet decomposition as an example, the original signal S can be expressed as:

$$S = cA_1 + cD_1 = cA_2 + cD_2 + cD_1 = cA_3 + cD_3 + cD_2 + cD_1 \quad (3)$$

where cA_j denotes the approximation coefficients obtained at the j level, representing the low-frequency components of the signal, and cD_j denotes the detail coefficients obtained at the j level, representing the high-frequency components. In most engineering signals, the useful information is primarily concentrated in the low- or mid-low-frequency bands, whereas random noise predominantly appears in the high-frequency components. Therefore, the detail coefficients cD_1, cD_2, cD_3, and often contain a significant amount of noise.

Let the monitored discrete signal be d, which is composed of the true signal f superimposed with noise ε. Applying wavelet decomposition to the vibration data, the linearity property of the wavelet transform yields:

$$W_0 d = W_0 f + W_0 \varepsilon \quad (4)$$

where W_0 denotes the wavelet transform operator, $f = [f_1, f_2, \dots, f_N]^T$ is the true signal vector, and ε is a Gaussian-distributed random noise vector. Therefore, the denoising problem consists of appropriately processing the noisy wavelet coefficients in the wavelet domain to recover the wavelet coefficients of the true signal. The core idea of wavelet threshold denoising is the thresholding of wavelet coefficients. Common methods include hard thresholding and soft thresholding, expressed as:

$$\eta_H(\omega,t) = \begin{cases}\omega & |\omega| \geq t \\ 0 & |\omega| < t\end{cases} \quad (5)$$

$$\eta_S(\omega,t) = \begin{cases}\omega - t & \omega \geq t \\ 0 & |\omega| < t \\ \omega + t & \omega \leq -t\end{cases} \quad (6)$$

where $\eta_H(\omega,t)$ and $\eta_S(\omega,t)$ denote the hard and soft threshold functions, respectively; ω is the wavelet coefficient, and t is the threshold parameter. A commonly used threshold selection is Donoho's universal threshold:

$$t = \varepsilon\sqrt{2\,ln\,N} \quad (7)$$

The soft threshold function is continuous, producing smoother denoising results, whereas the hard threshold function better preserves abrupt changes and peak features of the signal but may introduce ringing effects near coefficient boundaries [10].

After thresholding the wavelet coefficients, the denoised signal can be reconstructed via the inverse wavelet transform:

$$f^* = W_0^{-1}\eta(\cdot)W_0 d \quad (8)$$

where $\eta(\cdot)$ represents the thresholding operator. The wavelet-based denoising method, combining multi-scale decomposition with coefficient shrinkage, effectively suppresses noise while preserving local signal features, making it particularly suitable for processing non-stationary engineering signals.

ISSN: 2688-8645

2.2. Envelope Demodulation Denoising Method

Envelope demodulation is a vibration signal processing method based on modulation-demodulation theory, particularly suitable for detecting and identifying early weak fault features in low signal-to-noise ratio modulated signals [11, 12]. In engineering applications such as rotating machinery, bearing fault diagnosis, and magnetic flux leakage detection, fault information often exists in the form of low-frequency modulation on high-frequency carriers. The envelope demodulation method can effectively extract such modulated information. In practice, envelope demodulation is typically used as a preprocessing step for signal analysis. By extracting the signal envelope, high-frequency carrier components and part of the random noise are suppressed, which enhances the signal-to-noise ratio and produces a smoother signal, providing a clearer basis for subsequent spectral analysis or feature extraction.

Let $x(t)$ be the real-valued original monitored signal. Its Hilbert transform is defined as:

$$\hat{x}(t) = \mathcal{H}\{x(t)\} = \frac{1}{\pi} P.V. \int_{-\infty}^{+\infty} \frac{x(\tau)}{t-\tau} d\tau \tag{9}$$

where $\mathcal{H}\{\cdot\}$ denotes the Hilbert transform operator, and $P.V.$ represents the Cauchy principal value, which can be taken as 1. The physical meaning of the Hilbert transform is that a -90° phase shift is introduced to the positive frequency components and a $+90^{\circ}$ phase shift to the negative frequency components. Therefore, the Hilbert-transformed signal $\hat{x}(t)$ has the same amplitude spectrum and frequency components as the original signal $x(t)$, but is in quadrature (90° phase difference) with it [11, 13, 14, 15, 16].

Based on the Hilbert transform, the analytic signal of $x(t)$ can be constructed as:

$$g(t) = x(t) + j\hat{x}(t) \tag{10}$$

where j is the imaginary unit, and $g(t)$ is the corresponding analytic signal. The analytic signal contains only positive frequency components and can be represented as a rotating vector in the complex plane varying with time. The magnitude of the analytic signal, $|g(t)| = \sqrt{x^2(t) + \hat{x}^2(t)}$, is defined as the instantaneous envelope of the signal. The envelope reflects the amplitude variation of the modulated signal and effectively characterizes the low-frequency modulation information, while high-frequency carrier components are suppressed in the modulus operation, achieving partial attenuation of high-frequency noise and carrier signals. In a modulation signal model, the original vibration signal can be expressed as:

$$x(t) = [1 + m(t)] \cdot c(t) \tag{11}$$

where $m(t)$ is the low-frequency modulation signal containing fault features, and $c(t)$ is the high-frequency carrier signal. By constructing the analytic signal via the Hilbert transform and calculating its magnitude, the modulation information $m(t)$ is effectively demodulated and separated from the high-frequency carrier. Since noise generally exists as random high-frequency components, its energy is significantly weakened during envelope extraction. Therefore, the envelope demodulation method can achieve a certain level of denoising without significantly altering the original fault features.

3. Denoising Experiment and Analysis of Bearing Inner-Race Fault Signals

3.1. Data Selection

The locations of the measurement points are shown in Figure 1.

The bearing data were selected from the Case Western Reserve University (CWRU) Bearing Data Center, as shown in Figure 2. The data correspond to an inner-race fault with a fault size of 0.021 inches, collected under no-load conditions at a rotational speed of 1797 r/min. The sampling frequency was 12 kHz, and the data are provided in MATLAB format. The selected signals are the drive end accelerometer (DE) vibration data, as illustrated in Figure 1. The corresponding bearing model is SKF 6205 [3].

ISSN: 2688-8645

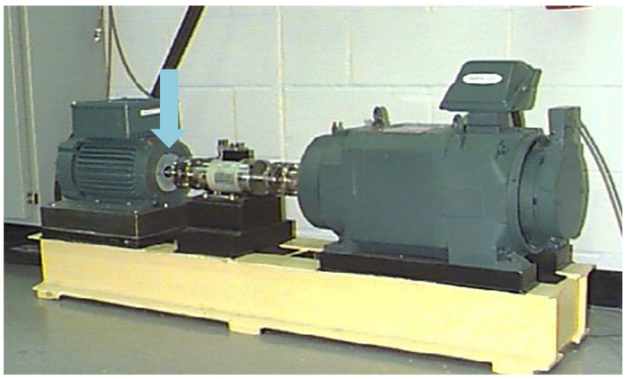

Figure 1. Schematic diagram of measurement point locations

Fault Diameter	Motor Load (HP)	Approx. Motor Speed (rpm)	Inner Race	Ball	Outer Race Position Relative to Load Zone (Load Zone Centered at 6:00)		
					Centered @6:00	Orthogonal @3:00	Opposite @12:00
0.007"	0	1797	IR007_0	B007_0	OR007@6_0	OR007@3_0	OR007@12_0
	1	1772	IR007_1	B007_1	OR007@6_1	OR007@3_1	OR007@12_1
	2	1750	IR007_2	B007_2	OR007@6_2	OR007@3_2	OR007@12_2
	3	1730	IR007_3	B007_3	OR007@6_3	OR007@3_3	OR007@12_3
0.014"	0	1797	IR014_0	B014_0	OR014@6_0	"	"
	1	1772	IR014_1	B014_1	OR014@6_1	"	"
	2	1750	IR014_2	B014_2	OR014@6_2	"	"
	3	1730	IR014_3	B014_3	OR014@6_3	"	"
0.021"	0	1797	IR021_0	B021_0	OR021@6_0	OR021@3_0	OR021@12_0

Figure 2. Data Selection

3.2. Time-Domain and Frequency-Domain Analysis of the Original Signal

As shown in Figures 3 and 4, the accelerometer has a relatively wide frequency response range, and the acquired signals can cover high-frequency components. Under normal instrument operation and field testing conditions, the original vibration signals inevitably contain a significant amount of high-frequency noise due to environmental vibrations, electromagnetic interference, and structural coupling. This results in a relatively low overall signal-to-noise ratio.

From the frequency spectrum analysis, the main effective component of the signal corresponds to a single fundamental frequency caused by bearing rotation, exhibiting a simple spectral structure with clear features. Although periodic variations can be observed in the time-domain signal, significant random fluctuations are present in the high-frequency region, indicating that high-frequency noise partially masks the fundamental frequency characteristics.

The rotational speed of the tested bearing is approximately *1797 r/min*, which corresponds to a rotational frequency of $f_r \approx 29.95Hz$. Considering slight fluctuations in rotational speed under actual operating conditions, as well as the effects of sensor installation, slip, and sampling errors, the fundamental frequency observed in the spectrum may deviate slightly from the theoretical value. Therefore, the fundamental frequency components are primarily distributed around the theoretical rotational frequency, with a deviation range of approximately *±10–20 Hz*. The spectral lines within this frequency band can serve as a reference for subsequent signal denoising and feature extraction.

3.3. Wavelet Denoising Method

In this experiment, a four-level wavelet packet decomposition is applied to denoise the bearing inner race fault signals, and the denoising performances of the soft-threshold and hard-

ISSN: 2688-8645

threshold methods are compared, respectively. A four-level wavelet decomposition is used for the wavelet packet analysis with both soft and hard thresholding, and the results are presented as follows.

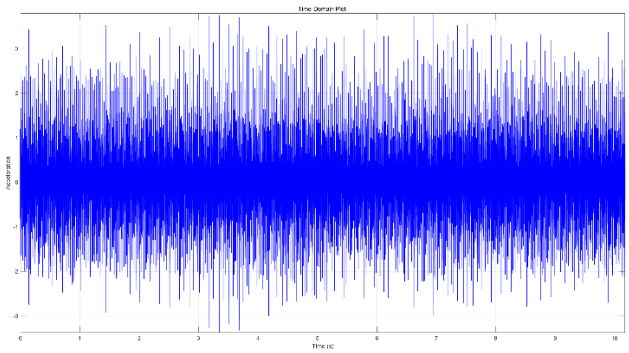

Figure 3. Time-domain waveform of the original signal

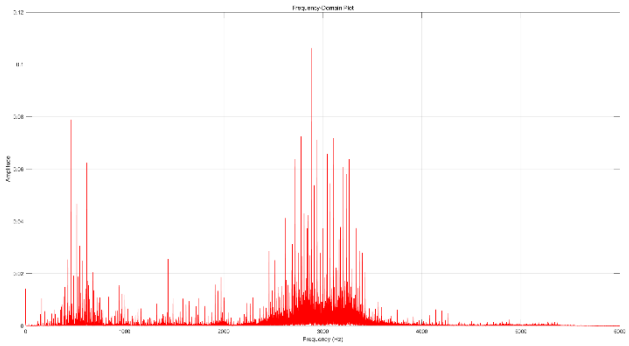

Figure 4. Frequency-domain spectrum of the original signal

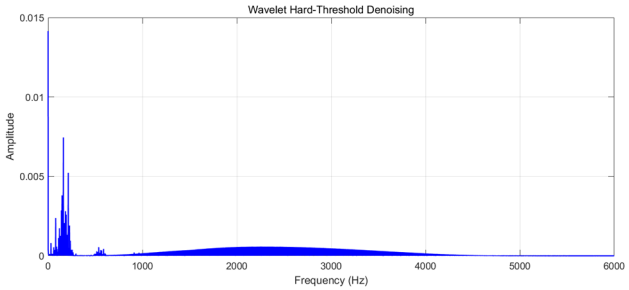

Figure 5. Spectrum after Wavelet Hard-Threshold Denoising

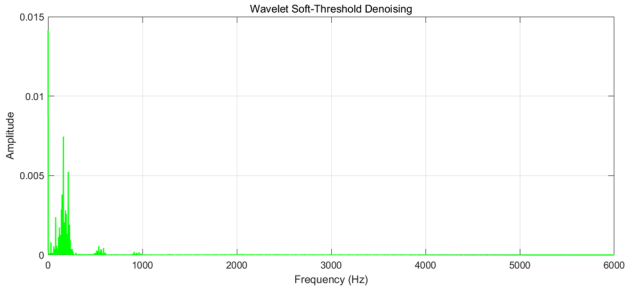

Figure 6. Spectrum after Wavelet Soft-Threshold Denoising

From the frequency spectrum analysis, it can be seen that after wavelet denoising, some characteristic peaks of the signal are observable; however, there still exist significant broadband noise components in the spectrum. This indicates that relying solely on wavelet

ISSN: 2688-8645

denoising is insufficient to effectively suppress the high-frequency noise in the acceleration signal. Comparing the effects of soft-threshold and hard-threshold wavelet denoising shows that the difference in overall denoising performance between the two methods is small. In particular, within the low-frequency characteristic bands, the impact on the main spectral structure is basically the same. Compared with hard-thresholding, wavelet soft-threshold denoising produces a certain smoothing effect on some high-frequency components in the *1000 Hz–2000 Hz* band, slightly reducing the spectral amplitude in this range, while noise components above this band remain relatively prominent. Therefore, wavelet threshold denoising has certain advantages in preserving the basic spectral characteristics of bearing signals, but its ability to suppress high-frequency random noise is limited. Especially when the signal-to-noise ratio is low, it is difficult to effectively enhance the useful fault characteristic frequencies.

3.4. Wavelet Envelope Demodulation Denoising Method

Based on the aforementioned envelope demodulation theory, the bearing vibration signals after Hilbert transform were subjected to wavelet denoising to compare their noise reduction performance. As shown in the analysis results of Figures 7 and 8, the use of the wavelet envelope demodulation method significantly improves the denoising effect of the vibration signals. Compared with the original signals, high-frequency noise components above 1000 Hz are effectively suppressed, and the spectral structure becomes clearer. In the envelope spectrum, the frequency component at 29.95 Hz exhibits a prominent peak, which corresponds to the theoretical rotational frequency of the bearing, and its spectral amplitude exceeds 0.05. This indicates that after denoising and demodulation, the fundamental frequency feature related to the bearing rotation is well preserved and enhanced. However, in the mid-frequency range of 300 Hz–2000 Hz, certain levels of noise interference still exist. The frequency components in this range are not sufficiently stable and do not clearly correspond to the bearing rotational frequency or its harmonics. Therefore, in subsequent fault feature extraction and analysis, this frequency band should be avoided as a criterion for identifying characteristic frequencies.

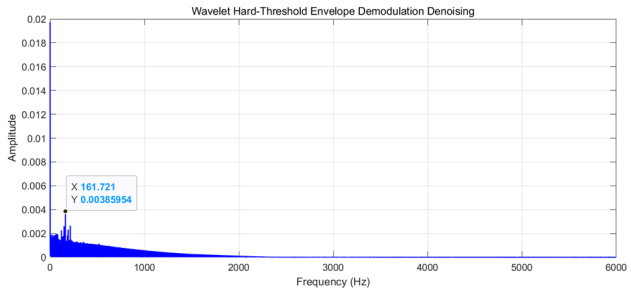

Figure 7. Spectrum after Wavelet Hard-Threshold Envelope Demodulation Denoising

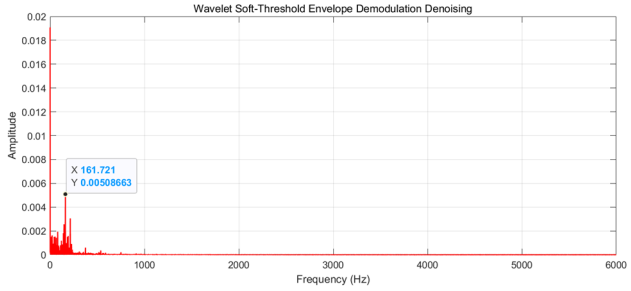

Figure 8. Spectrum after Wavelet Soft-Threshold Envelope Demodulation Denoising

The bearing characteristic frequency coefficients are listed in Table 1 [17, 18]. The theoretical inner race characteristic frequency is calculated as:

ISSN: 2688-8645

$$\mathrm{BPFI} = 1797 \div 60 \times 5.4152 = 162.104\mathrm{Hz} \quad (12)$$

which is basically consistent with the result of *161.721* Hz obtained after wavelet envelope demodulation denoising, with an error of approximately *0.236%*.

By comparing the wavelet threshold denoising methods, it can be seen that whether using hard-threshold or soft-threshold processing, the difference in their impact on the overall signal characteristics is small. Both methods are less effective than wavelet envelope demodulation in highlighting low-frequency modulation features.

Table 1. Bearing Fault Characteristic Frequency Factors

Inner Race	Outer Race	Cage	Rolling Element
5.4152	3.5848	0.39828	4.7135

4. Conclusion

From the comparative experimental analysis of wavelet threshold denoising and wavelet envelope demodulation denoising methods, it can be concluded that when preprocessing bearing vibration signals acquired by acceleration sensors, performing wavelet denoising on top of envelope demodulation can achieve better signal smoothing and noise reduction. The analytic signal obtained via Hilbert transform effectively extracts the amplitude modulation information in the vibration signal, making the low-frequency features related to bearing rotation more prominent and providing a solid foundation for subsequent wavelet denoising. Considering the wideband acquisition characteristics of the acceleration sensors and the noise distribution under actual operating conditions, a comparative analysis of the time-domain waveforms and frequency spectra shows that the combined method of envelope demodulation and wavelet denoising can effectively suppress high-frequency noise while preserving key features such as the bearing rotational frequency. This significantly improves the signal-to-noise ratio and the distinguishability of characteristic features. The results indicate that proper denoising preprocessing of bearing vibration signals is of great significance for highlighting characteristic frequencies related to equipment operating conditions. The vibration signals processed by the aforementioned method can be further used for bearing fault feature extraction and condition identification, providing reliable data support for rapid and accurate diagnosis of equipment anomalies and faults.

References

[1] H.W. Zhang, K. Tang, L. He, et al.: Research on Fault Diagnosis and Prevention Technology of Railway Vehicle Bearings (Shidai Qiche, 2023, No.19, p.169-171). (In Chinese)

[2] Y. Cai, B.H. Jia, X.G. Shi: Diagnosis of Typical Vibration Faults of A320 Aircraft (Journal of Civil Aviation University of China, 2004, S1, p.7-9). (In Chinese)

[3] Bearing Data Center | Case School of Engineering | Case Western Reserve University [EB/OL]. Available: https://engineering.case.edu/bearingdatacenter

[4] F. Ding, F.W. Qin: Application Research of Wavelet Transform in Motor Fault Diagnosis and Testing (Journal of Electrical Machines and Control, 2017, 21(06), p.89-95). (In Chinese)

[5] P.M. Shi, S. Xu, P. Li: Rolling Bearing Fault Diagnosis Method Based on Wavelet Denoising and EEMD Envelope Analysis (Xiandai Zhizao Gongcheng / Modern Manufacturing Engineering, 2015, No.12, p.12-17). (In Chinese)

[6] L.J. Meng, J.W. Xiang, Y. Zhong, et al.: Fault Diagnosis of Rolling Bearing Based on Second Generation Wavelet Denoising and Morphological Filter (Journal of Mechanical Engineering, 2014, 29(8)).

[7] X.Y. Gong, C.Y. Yang, J. Han, et al.: Full Information Demodulation Method Based on Wavelet Packet and Its Application (Journal of Vibration, Measurement and Diagnosis, 2014, 34(04), p.668-672, 777). (In Chinese)

[8] F.L. Yao, X. Yang, F.Z. Ding, et al.: Research on Rolling Bearing Fault Diagnosis Technology Based on Wavelet Analysis (Zhizao Jishu yu Jichuang / Manufacturing Technology and Machine Tools, 2023, No.07, p.16-20, 31). (In Chinese)

[9] J. Ma, K. Li, Y. Tian, et al.: Research on Wavelet Denoising Algorithm for Metal Chip Signals Based on Kurtosis [C]// Proceedings of the 20th Annual Conference on Aerospace Measurement and Control Technology, 2023, p.143-146. (In Chinese)

[10] W.H. Li: Research and Application of Bearing Fault Diagnosis System for Wind Turbines (Ph.D., North China Electric Power University, China, 2017). (In Chinese)

[11] J.C. Guo, Z.Q. Shi, D. Zhen, et al.: Modulation Signal Bispectrum with Optimized Wavelet Packet Denoising for Rolling Bearing Fault Diagnosis (Structural Health Monitoring, 2021, 21(3), p.984-1011).

[12] Z.C. Cai: Vibration Detection and Fault Diagnosis of Wind Turbine Bearings (Ph.D., North China Electric Power University, China, 2014). (In Chinese)

[13] E.M. Bertot, P. Beaujean, D. Vendittis, et al.: Refining Envelope Analysis Methods Using Wavelet De-Noising to Identify Bearing Faults (2014, p.1-8).

[14] M. Alonso-González, V.-G. Díaz, B.-L. Pérez, et al.: Bearing Fault Diagnosis with Envelope Analysis and Machine Learning Approaches Using CWRU Dataset (IEEE Access, 2023, 11, p.57796-57805).

[15] X. Li, J. Ma, X. Wang, et al.: An Improved Local Mean Decomposition Method Based on Improved Composite Interpolation Envelope and Its Application in Bearing Fault Feature Extraction (ISA Transactions, 2020, 97, p.365-383).

[16] R.A. Cottis, A.M. Homborg, J.M.C. Mol: The Relationship Between Spectral and Wavelet Techniques for Noise Analysis (Electrochimica Acta, 2016, 202, p.277-287).

[17] A. Darji, D. Pandya: Fault Diagnosis of SKF-6205 Bearing with Modified Empirical Mode Decomposition (International Journal of Engineering, Science and Technology, 2022, 13, p.12-20).

[18] D.X. Cheng: Mechanical Design Handbook—Bearings (2017, No.12, p.86-87). (In Chinese)